

**EXPERIMENTAL AND THEORETICAL INVESTIGATION OF
SURFACE CHEMISTRY INDUCED BY DIRECT AND INDIRECT ELECTRONIC
EXCITATION**

Peter C. Stair and Eric Weitz
Department of Chemistry
Northwestern University
Evanston, Illinois 60208

July 1993

Final Report for September 1991 to March 1993
Contract Number: AFOSR-91-0377

DISTRIBUTION UNLIMITED

Prepared for

AIR FORCE OFFICE OF SCIENTIFIC RESEARCH
Bolling Air Force Base, D.C. 20332-6448

Accession For	
NTIS CRA&I	<input checked="" type="checkbox"/>
DTIC TAB	<input type="checkbox"/>
Unannounced	<input type="checkbox"/>
Justification	
By	
Distribution/	
Availability Codes	
Dist	Avail and/or Special
A-1	

Abstract

The ultraviolet (uv) photodissociation and photodesorption of CD₃I adsorbed on the TiO₂(110) surface at ~100 K has been investigated at 257, 275, 302 and 351 nm using modulated continuous-wave (cw) laser irradiation followed by resonantly enhanced multiphoton ionization (REMPI) of fragments expelled from the adsorbate layer. Photodissociation at these wavelengths produces CD₃ radicals. Non-thermal photodesorption also contributes to removal of CD₃I from the adsorbate layer, becoming a major mechanism at 351 nm. Similar processes are observed at both 1 and 25 monolayer (ML) coverages. The cross-section for CD₃I depletion from the monolayer is qualitatively similar to the gas phase CD₃I absorption profile, decreasing by ~3 orders of magnitude between 257 and 351 nm. We calculate depletion cross-sections, S, of $3\pm 2\times 10^{-18}$ cm⁻², $8\pm 3\times 10^{-19}$ cm⁻², $1\pm 0.5\times 10^{-19}$ cm⁻² and $3\pm 1\times 10^{-21}$ cm⁻² for 257, 275, 302 and 351 nm irradiation respectively. However, the depletion cross-section for 25 ML CD₃I coverage is approximately an order of magnitude less than for 1 ML coverage with S calculated to be $3\pm 2\times 10^{-19}$ cm⁻², $1.5\pm 0.7\times 10^{-19}$ cm⁻², $1.5\pm 0.7\times 10^{-20}$ cm⁻² and $2\pm 0.8\times 10^{-22}$ cm⁻² for 257, 275, 302 and 351 nm radiation respectively. We find no correlation between substrate absorption and the wavelength dependence of photodissociation or photodesorption suggesting that direct excitation of the adsorbate molecule is the dominant dissociation mechanism. The lack of substrate involvement may be due to poor overlap of the CD₃I lowest unoccupied molecular orbital (LUMO) with the range of sub-vacuum level electron energies expected to be produced at these wavelengths.

Introduction

There is now a considerable body of work concerned with the uv photochemistry of molecules adsorbed on well characterized metal, and to a lesser extent, semiconductor and insulator surfaces. Several detailed review articles have already appeared on this subject¹⁻³. It has become clear that the photochemistry of monolayer adsorbates on surfaces is strongly influenced by a competition between promotion of the molecule to an excited state and quenching of that excited state. Excitation can be driven either by adsorbate or substrate photon absorption, and depending upon the excited state lifetime, a variety of relaxation mechanisms (quenching) may be important. These include radiative processes (fluorescence and phosphorescence), non-radiative processes (energy transfer to the surface or neighboring molecules *via* excitation of plasmons, phonons or creation of electron-hole pairs) and chemical reaction. As a result, extensive modification of photochemical behavior has been observed for an adsorbate molecule with respect to its gas phase counterpart. Clearly, knowledge of the adsorbate-substrate interaction is crucial for understanding these systems, and elaboration of the important excitation and quenching mechanisms will enable one to describe and predict photochemical behavior for adsorbates on solid surfaces.

We present here an investigation of the photochemistry of CD₃I adsorbed on TiO₂(110) at ~100 K at four uv wavelengths: 257, 275, 302 and 351 nm. Experiments were also attempted at 458 nm. We anticipate sub-vacuum level carriers will be produced in the absence of photoelectrons and expect CD₃I to exhibit some absorption in the 257-351 nm wavelength range. In systems where photochemistry is the result of substrate mediated excitation, it has been demonstrated that hot carriers generated at the substrate surface have a limited effective range

in thick adsorbate layers, and these surface effects are lost when the adsorbate is separated from the surface by "spacer layers" of molecules⁴. Therefore, if photodissociation is confined to the outermost layers of an adsorbate film, the layers of molecules closest to the surface would not significantly contribute to the observed photochemistry. Thus, by examining CD₃I photodesorption and photodissociation as a function of wavelength at different coverages, we hope to distinguish the influence of surface mediated sub-vacuum excitation processes, most likely to be evident at monolayer CD₃I coverage, from the excitation mechanisms dominant in solid-like CD₃I films as expected at thick multilayer coverages.

Experimental

A diagram of the ultra-high vacuum (UHV)/laser system used in this work is shown in Fig. 1. A detailed description has been published elsewhere⁵, but a brief outline is given below. A cw Ar ion laser provided photolysis radiation at 458, 351, 302 or 275 nm. 257 nm radiation was generated by frequency doubling the 514 nm line. An acousto-optical modulator (AOM) was used to produce a variable duration photolysis "pulse" (≥ 200 ns) which was focussed onto the TiO₂(100) surface by a $f/20$ quartz lens. The use of a modulated cw photolysis source allows the continuous sampling of photofragments with a broad translational energy distribution without the need for repetitive incremental photolysis-probe delay experiments as is commonly employed in experiments using two pulsed lasers⁶. The beam intersects the sample at 45° from the surface normal creating an ellipsoidal irradiated area. The surface normal coincides with the detection axis of a single stage time-of-flight mass spectrometer (TOF-MS) described later. The spatial intensity profile of a noble gas ion laser operating in the lowest order transverse electromagnetic mode (TEM₀₀) is approximately Gaussian^{7,8}. The beam width at the surface, w_x (ellipse major axis), was experimentally determined by using an auto-correlation method⁹. This procedure involved irradiating the adsorbate layer until the CD₃⁺ signal fell to ~10% of its initial intensity and then translating the sample in small increments until the signal intensity returned to its initial value, the distance moved being approximately equal to w_x . Typical values for w_x were 200-300 μm . A half-order wave plate was used to rotate the photolysis laser polarization so that the photon electric vector **E** was 45° from the surface normal, and in the crystal (010) direction. Laser power, measured at the MgF₂ entrance window to the UHV chamber, was typically 2-5 mW at $\lambda=257$ and 275 nm, 30-40 mW at $\lambda=302$ nm, 70-80 mW at $\lambda=351$ nm and 25-35 mW

at 458 nm. Higher fluences were necessary at longer wavelengths to compensate for decreased dissociation and desorption efficiencies.

CD₃ photofragments produced by irradiation of the CD₃I adsorbate were ionized, after a short delay following cessation of the photolysis pulse (2-4 μs), by a tuneable uv probe laser (excimer-pumped dye laser system, 1-2.5 mJ pulse⁻¹ in the frequency doubled output) *via* resonantly enhanced multi-photon ionization (REMPI) at ~333.7 nm. A f8 lens inside the UHV chamber was used to produce a tight focal volume ~5-8 mm directly over the photolysis area and along the TOF-MS axis. Positively charged ions created by the probe laser were accelerated by a positive potential (+1000 V) continuously applied to the first grid of the TOF-MS, labelled G1 in Fig. 1. The surface was positioned 0.5-1 mm from G1. Ions were separated according to their mass-to-charge ratio (m/e) in a field-free region bounded by two grounded grids, G2 and G3, detected by a micro-channel plate (MCP) detector, and counted using a preamplifier/discriminator/digital storage oscilloscope (DSO). Signals from 500 to 5,000 laser shots were typically averaged.

The back of a polished TiO₂ crystal, approximately 6x3x1 mm, was cemented to Ni foil using a high temperature Ag/glass amalgam. Ni wires were spot-welded to the Ni foil to allow attachment of the crystal mount assembly to a standard UHV manipulator with facilities for liquid N₂ cooling to ~100 K and heating to 1000 K by electron bombardment from a W filament behind the Ni foil. Surface temperature was measured by a chromel-alumel thermocouple cemented to the edge of the crystal as close to the front surface as possible. A clean (110) surface was prepared *in vacuo* by cycles of Ar⁺ sputtering (1-2 keV, 20 μA cm⁻²) and subsequent annealing in 3x10⁻⁶ torr O₂ at 1000 K (60-120 minutes). Such a procedure reproducibly generates clean,

ordered and stoichiometric surfaces as determined by Auger electron spectroscopy (AES)¹⁰, X-ray photoelectron spectroscopy (XPS)¹¹ and low energy electron diffraction (LEED)¹². In this work, AES was used to characterize the surface, but its use was minimized to avoid electron beam reduction of the surface. The establishment of a clean, fully oxidized TiO₂(110) surface was gauged from the AES Ti LMM and O KVV peak intensities and from the Ti LMM peak shape¹³. The surface prepared by this method, was cooled to 100±5 K and dosed by admitting CD₃I into the UHV chamber at pressures up to 10⁻⁷ Torr as appropriate. Exposures in Langmuirs (L) were calculated by integrating an ion gauge signal (~150 mm from the surface) over the dosing duration without correcting for ionization efficiency.

The adsorption behavior of CD₃I on TiO₂(110) has been investigated using TPD and XPS and the results will be presented elsewhere¹⁴. It is sufficient to comment here that CD₃I adsorbs molecularly on TiO₂(110): monolayer coverage forming at less than ~170 K and multilayers forming at less than ~140 K. The monolayer coverage used in this work corresponds to ~3.8×10¹⁴ molecules cm⁻² and an exposure of 3.3 L (1 L≡10⁻⁶ Torr-sec). The multilayer coverage corresponds to 25±3 ML. Additionally, thermal dissociation of CD₃I on the TiO₂(110) surface was not observed at any time during TPD measurements.

Conclusions

Irradiation of both monolayer and multilayer CD₃I coverages on TiO₂ at 100 K in the wavelength range 275-351 nm generates CD₃ radicals as a result of direct dissociation within the adsorbate layer. A photodepletion cross-section calculated for removal of the CD₃I from the adlayer shows similar wavelength behavior to the gas phase molecule photodissociation cross-

section at 257 and 275 nm, but there is some enhancement over the gas phase value at 302 and 351 nm. Similar behavior of the CD₃I photodepletion cross-section is observed for both 1 ML and 25 ML CD₃I coverages implying that a similar photodissociation mechanism dominates in both cases. However, the multilayer depletion cross-section is consistently ~1 order of magnitude below the monolayer data. This may indicate that efficient caging effects are operating in the multilayer regime. Further experiments are underway to investigate this phenomenon. Photodesorption does not appear to be due to either bulk or transient surface heating effects (excitation by phonons). The calculated surface temperature rise for TiO₂, largest at the high power densities used at 351 nm, is less than 3 K. Desorption of the parent molecule is a non-thermal process and desorption is a relatively minor CD₃I depletion mechanism at the power densities used in this work except at 351 nm for 25 ML coverage. Both dissociation and desorption are single photon events at the incident power densities used here and we speculate that adsorbate photodissociation proceeds in a similar manner to the gas phase molecule at the shorter uv wavelengths used in this work (*ie* a single photon absorption prepares an excited adsorbate molecule which promptly dissociates). Quenching of the excited adsorbate by the TiO₂(110) appears to be unable to compete with the dissociation event.

The wavelength behavior of adsorbed CD₃I photodissociation most closely follows the gas phase absorption profile of CD₃I and does not appear to correlate with the TiO₂(110) absorption profile. There is no evidence that photodissociation and photodesorption behavior observed in this system is dominated by surface excitation, although sub-vacuum level carriers are expected to be produced in TiO₂ in the absence of photoelectrons at all the wavelengths studied. The relevant energy level diagram for this system is shown in Fig. 2. The CD₃I LUMO is positioned

in the band-gap, approximately 0.4 eV above the TiO₂ Fermi level but about 0.4 eV below the bottom of the TiO₂ conduction band. The most energetic photons used in this work (257 nm) are capable of generating electrons with energies from the bottom of the conduction band up to 2.6 eV above the Fermi level of TiO₂, but the position of the CD₃I LUMO in the band-gap means that photo-generated electrons in the substrate have a low probability of tunnelling into the CD₃I LUMO, and therefore the photochemistry of CD₃I will not be significantly influenced by substrate excitation.

It is possible that the wavelength dependence of the photochemistry of CD₃I on the TiO₂(110) surface is the combined result of direct adsorbate and substrate mediated processes. At the shorter uv wavelengths used in this work (257 and 275 nm), CD₃I dissociation is dominated by direct adsorbate absorption since the values of $S_{\text{monolayer}}$ and the gas phase dissociation cross-section σ are very similar. The enhancement of $S_{\text{monolayer}}$ with respect to σ which is observed at 302 nm and at 351 nm, may be due to a relatively weak substrate mediated process which shows a less pronounced wavelength behaviour expected for the carrier function $(1-R(\omega))(1-e^{-\alpha d})$ compared to the CD₃I absorption profile. Within the context of this model, the surface process becomes most significant at 351 nm where the adsorbate absorption is weakest. The availability of an absorption spectrum of a cold CD₃I solid film would help resolve this issue.

Personnel

Principal Investigators: Professor Peter C. Stair
Professor Eric Weitz

Postdoctoral Research Associates: Simon J. Garrett

Graduate Students: Victor P. Holbert

Publications

- (1) Wavelength dependence of the photodissociation and photodesorption of CD₃I adsorbed on the TiO₂(110) surface.
S.J. Garrett, V.P. Holbert, P.C. Stair and E. Weitz, submitted to J. Chem. Phys.
- (2) Adsorption and photochemistry of CD₃I on TiO₂(110): An investigation by x-ray photoelectron spectroscopy and temperature programmed desorption.
S.J. Garrett, V.P. Holbert, P.C. Stair and E. Weitz, submitted to J. Chem. Phys.
- (3) A comparison of multiphoton ionization mechanisms in CH₃I and CD₃I
S. J. Garrett, V. P. Holbert, D. H. Fairbrother, P. C. Stair and E. Weitz, submitted to Chem. Phys. Lett.
- (4) The dynamics of adsorbed molecule photodissociation: the 257-nm photolysis of CD₃I on TiO₂(110).
V. P. Holbert, S. J. Garrett, P. C. Stair and E. Weitz, in preparation.
- (5) The dynamics of adsorbed molecule photodissociation: the wavelength dependent photolysis of CD₃I on TiO₂(110).
V. P. Holbert, S. J. Garrett, P. C. Stair and E. Weitz, in preparation.

Presentations

Photodissociation of CD₃I and CH₃I on TiO₂(110) and MgO(100) surfaces under UHV conditions.
Eric Weitz
University of Southern California, October 1991.
American Chemical Society Meeting, Washington, D.C., August 1992.

References

1. X.L. Zhou, X.Y. Zhu, J.M. White, *Surf. Sci. Rep.* **13**, 73 (1991).
2. J.C. Polanyi, H. Rieley in *Dynamics of Gas-Surface Interactions*, edited by C.T. Rettner, M.N.R. Ashfold (Royal Society of Chemistry, London, 1991).
3. S.R. Meech in *Photochemistry Volume 23*, edited by D. Bryce-Smith, A. Gilbert (Royal Society of Chemistry, London, 1992).
4. S.K. Jo, J.M. White, *J. Chem. Phys.* **94**, 5671 (1991).
5. K.A. Trentelman, H. Fairbrother, P.C. Stair, P.G. Strupp, E. Weitz, *J. Vac. Sci. Technol.* **A 9**, 1820 (1991).
6. K.A. Trentelman, D.H. Fairbrother, P.G. Strupp, P.C. Stair, E. Weitz, *J. Chem. Phys.* **96**, 9221 (1992).
7. J.P. Campbell, L.G. DeShazer, *J. Opt. Soc. Am.* **59**, 1427 (1969).
8. R.G. Schell, G. Tyras, *J. Opt. Soc. Am.* **61**, 31 (1971).
9. S.M. George, A. M. DeSantolo, R.B. Hall, *Surf. Sci.* **159**, L425 (1985).
10. N.R. Armstrong, R.K. Quinn, *Surf. Sci.* **67**, 451 (1977).
11. W. Gopel, G. Rocker, R. Feierabend, *Phys. Rev. B* **28**, 3427 (1983).
12. L.E. Firment, *Surf. Sci.* **116**, 205 (1982).
13. J.S. Soloman, W.L. Baun, *Surf. Sci.* **51**, 228 (1975).
14. S.J. Garrett, V.P. Holbert, P.C. Stair, E. Weitz, to be published.

Wavelength (nm)	σ_{gas} (cm ⁻²)	$S_{\text{monolayer}}$ (cm ⁻²)	$S_{\text{multilayer}}$ (cm ⁻²)
257	1.5×10^{-18}	$3.0 \pm 2.0 \times 10^{-18}$	$3.0 \pm 2.0 \times 10^{-19}$
275	5×10^{-19}	$8.0 \pm 3.0 \times 10^{-19}$	$1.5 \pm 0.7 \times 10^{-19}$
302	6×10^{-20}	$1.0 \pm 0.5 \times 10^{-19}$	$1.5 \pm 0.7 \times 10^{-20}$
351	$1 \times 10^{-22\dagger}$	$3.0 \pm 1.0 \times 10^{-21}$	$2.0 \pm 0.8 \times 10^{-22}$
458	-	$< 1.0 \times 10^{-23}$	-

Table 1: CD₃I depletion cross-sections S calculated from least squares fits to depletion curves using a Gaussian beam modified first order depletion process. Gas phase values of the dissociation cross-section σ are also included³⁷.

† Estimated by extrapolation.

Figure Captions

Fig. 1 Experimental UHV chamber/laser system used to probe the photofragments expelled from irradiated CD₃I adsorbed on TiO₂(110) at ~100 K by time-of-flight detection. Shown is the arrangement for a 257 nm photolysis source provided by modulating the frequency doubled cw output of an Ar ion laser. The appropriate probe laser wavelength was provided by an excimer-pumped dye laser system.

Fig. 2 Suggested energy level diagram for CD₃I adsorbed on TiO₂(110). The TiO₂ vacuum level is shown without correction for changes in the workfunction caused by CD₃I adsorption and the CD₃I energy levels correspond to the gas phase molecular orbitals. The shaded area represents the range of electron energies expected to be produced in this working using uv wavelengths ≥ 257 nm.

Figure 1

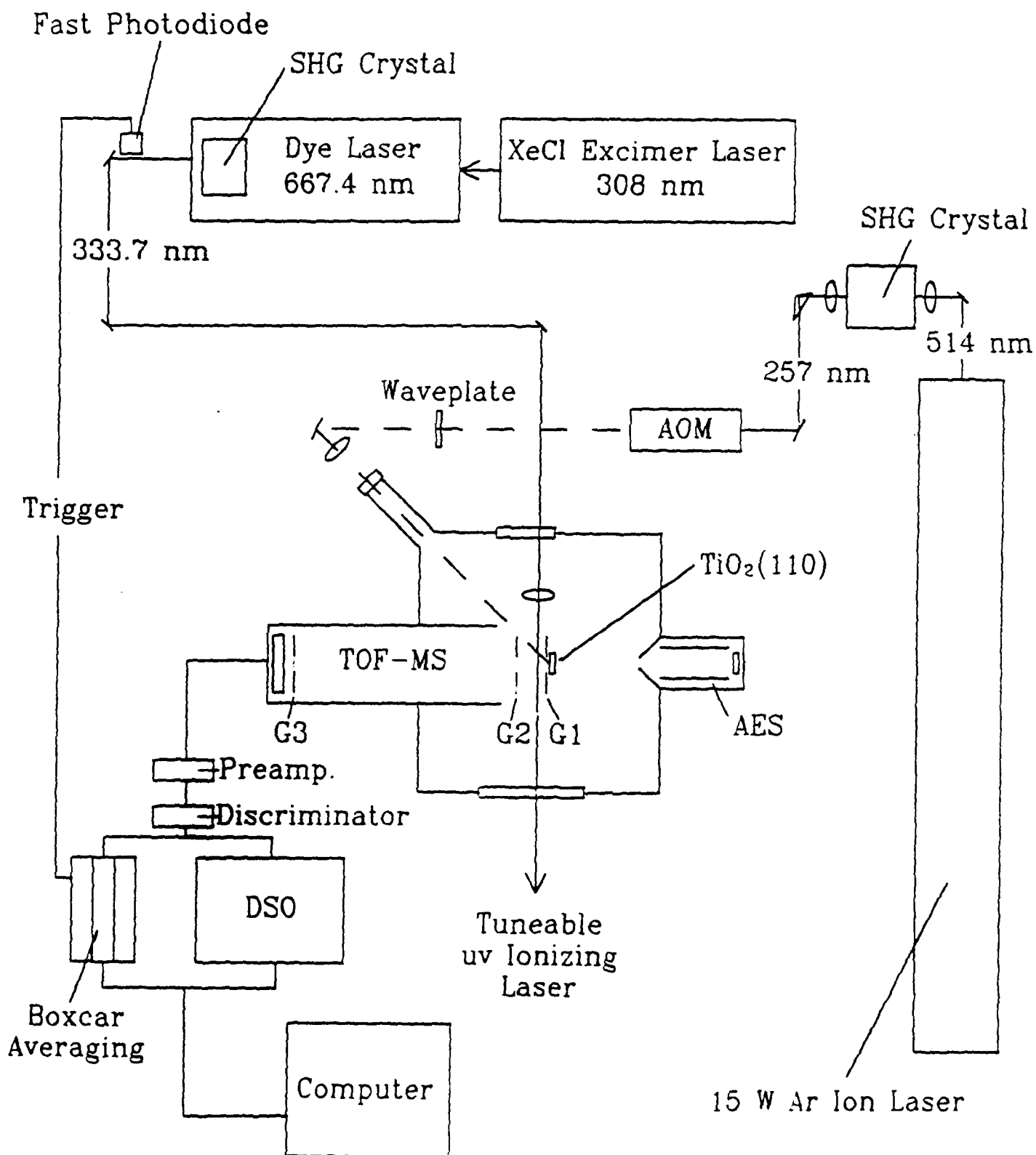


Figure 2

